Palm Vein Extraction and Matching for Personal Authentication

Yi-Bo Zhang[1], Qin Li[2], Jane You[2], and Prabir Bhattacharya[1]

[1] Institute for Information Systems Engineering, Concordia University, Quebec, Canada
prabir@ciise.concordia.ca
[2] Biometrics Research Centre, Department of Computing, The Hong Kong Polytechnic University, KLN, Hong Kong
{csqinli,csyjia}@comp.polyu.edu.hk

Abstract. In this paper, we propose a scheme of personal authentication using palm vein. The infrared palm images which contain the palm vein information are used for our system. Because the vein information represents the liveness of a human, this system can provide personal authentication and liveness detection concurrently. The proposed system include: 1) Infrared palm images capture; 2) Detection of Region of Interest; 3) Palm vein extraction by multiscale filtering; 4) Matching. The experimental results demonstrate that the recognition rate using palm vein is good.

Keywords: Palm vein, Personal identification, Liveness detection, Infrared palm images, Multiscale filtering.

1 Introduction

The personal identification using hand and palm vein has gained more and more research attentions these years [1] [2] [3] [4] [5]. There are many good properties of this kind of biometric feature: 1) the vein information can represent the liveness of an object; 2) it is difficult to be damaged and modified as an internal feature; 3) it is difficult to simulated using a fake palm. Because of these, hand and palm vein seems a better biometric feature that finger print and face.

In [1] [2], the thermal images are used to extract palm vein and obtained good results. But the infrared thermal camera is very expensive. In [5], a low cost CCD camera is used to capture near infrared image of palm. That system's recognition rate is good. But because both vein and texture information are used in [5] for recognition, that method can not ensure the liveness of a person.

In this work, we use a low cost CCD camera to capture the infrared palm images. The palm vein, rather than hand vein (back of the hand), is used by our system because it is easier to deign a platform to help a user fixing his/her hand on the image capture device. And, we only use the palm vein as biometric feature without any other features such as palm texture and palm line so that this system can ensure the liveness of an object.

G. Qiu et al. (Eds.): VISUAL 2007, LNCS 4781, pp. 154–164, 2007.
© Springer-Verlag Berlin Heidelberg 2007

2 Image Capture and ROI Locating

The capture device is modified from our previous work on palmprint [6]. Fig. 1 shows part of our device. There are three poles to help a user to fix his/her hand (Fig. 1(b)). A low cost CCD camera is used in this system. In order to obtain infrared images, a set of infrared light source is installed around the camera.

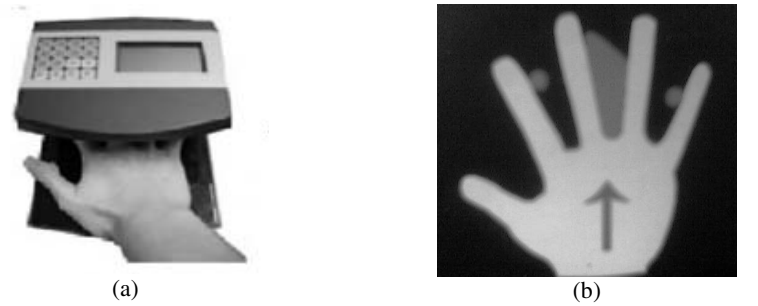

(a) (b)

Fig. 1. Capture device. (a) outside of the device; (b) poles to fix a palm.

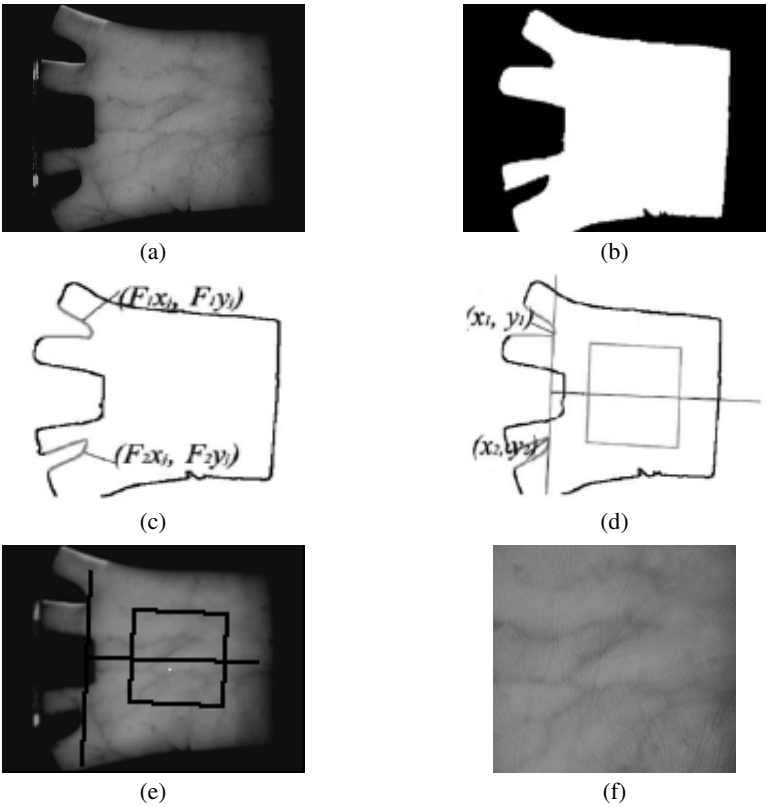

(a) (b)

(c) (d)

(e) (f)

Fig. 2. Locate ROI. (a) a infrared palm image captured by our device; (b) binarized image; (c) boundaries; (d) and (e) ROI locating; (f) the subimage in ROI.

After image capture, the region of interest (ROI) is located by the same method of our previous work [6]. A small area (128*128 pixels) of a palm image is located as ROI to extract the features and to compare different palms. Using the features within ROI for recognition can improve the computation efficiency significantly. Further, because this ROI is located by a normalized coordinate based on the palm boundaries, the recognition error caused by a user who slightly rotate or shift his/her hand is minimized. Figure 2 illustrates the procedure of ROI locating:

1). Binarize the input image (Fig. 2(a) and (b));
2). Obtain the boundaries of the gaps, (Fixj;Fiyj) (Fig. 2(c));
3). Compute the tangent of the two gaps (Fig. 2(d)), use this tangent (the line connect (x1,y1) and (x2,y2)) as the Y-axis of the palm coordinate;
4). Use a line passing through the midpoint of the two points (x1,y1) and (x2,y2), which is also perpendicular to the Y-axis, as the X-axis (the line perpendicular to the tangent in Fig. 2(d));
5). The ROI is located as a square of fixed size whose center has a fixed distance to the palm coordinate origin (Fig. 2(d) and (e));
6). Extract the subimage within the ROI (Fig. 2(e) and (f)).

3 Palm Vein Extraction

By observing the cross-sections of palm veins, we found that they are Gaussian-shaped lines. Fig. 3 shows some cross-sections of the palm veins. Based on this observation, the matched filter proposed in [7] [8] can be used to detect palm veins. And, we propose a multiscale scheme to improve the performance of vein detection. This scheme includes multiscale matched filters and scale production [9] [10] [11].

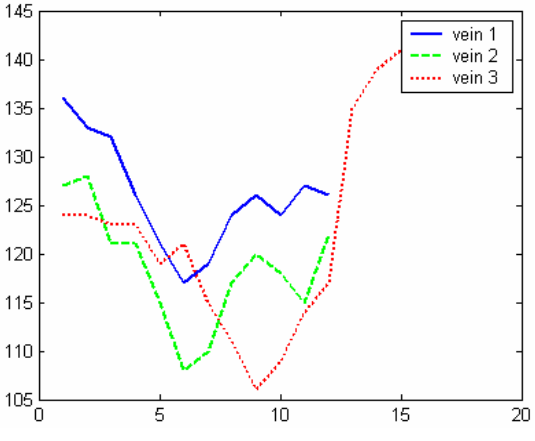

Fig. 3. Cross section evaluation

The matched filter was defined as

$$\begin{cases} g_{\phi}(x,y) = -\exp\left(-x'^2/\sigma_x^{\,2}\right) - m, & \text{for } |x'| \le 3\sigma_x, \quad |y'| \le L/2 \\ x' = x\cos\phi + y\sin\phi \\ y' = y\cos\phi - x\sin\phi \end{cases} \tag{1}$$

where ϕ is the filter direction, σ is standard deviation of Gaussian, m is the mean value of the filter, L is the length of the filter in y direction which is set according to experience. This filter can be regarded as Gaussian filter in x direction. A Gaussian-shaped filter can help to denoise and the zero-sum can help to suppress the background pixels. Fig. 4 shows the matched filters in 1-D (a) and 2-D (b) view. Fig. 5 gives the filter response in a single scale.

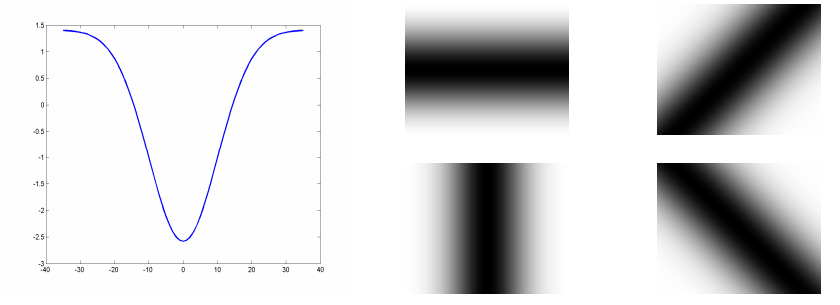

Fig. 4. Matched filters (a) 1-D and (b) 2-D

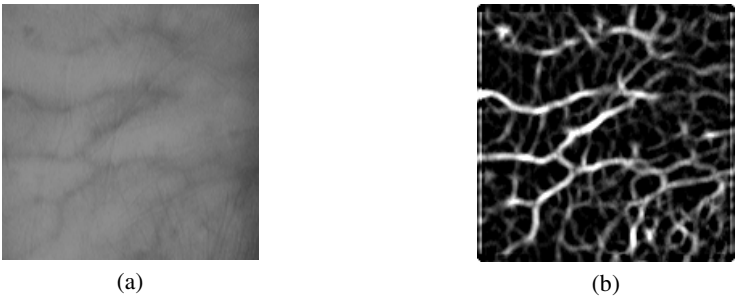

(a) (b)

Fig. 5. (a) The subimage within ROI and (b) its single scale Matched filter response

From Fig. 5, we find that there is too much noise in the matched filter responses of infrared palm images. To gain a proper signal-noise ratio, we propose a multiscale scheme to detect the palm vein. In [12], Mallat illustrated mathematically that signals and noise have different singularities and that edge structures present observable magnitudes along the scales, while noise decreases rapidly. With this observation, we

responded to those problems of edge and line detection and noise reduction by thresholding the multiscale products [9] [10] [11]. For Multiscale analysis, a scale parameter is added to equation (1) to control the filter size:

$$g_{\phi,s}(x,y) = -\exp\left(-x'^2 / s\sigma_x^2\right) - m, \quad \text{for } |x'| \le 3s\sigma_x, \quad |y'| \le sL/2 \tag{2}$$

The response of multiscale matched filter can be expressed by

$$R_g(x,y) = g_{\phi,s}(x,y) * f(x,y) \tag{3}$$

where $f(x,y)$ is the original image and $*$ denotes convolution.

The scale production is defined as the product of filter responses at two adjacent scales

$$P^{s_j}(x,y) = R_g^{s_j}(x,y) \cdot R_g^{s_{j+1}}(x,y) \tag{4}$$

Fig. 6 illustrates the multiscale line detection and scale production, where Mf1 and Mf2 are the responses at two different scales, P1,2 is their production. The noise in Mf1 and Mf2 nearly reaches the half peak of the signal response. After production, the noise becomes much smaller.

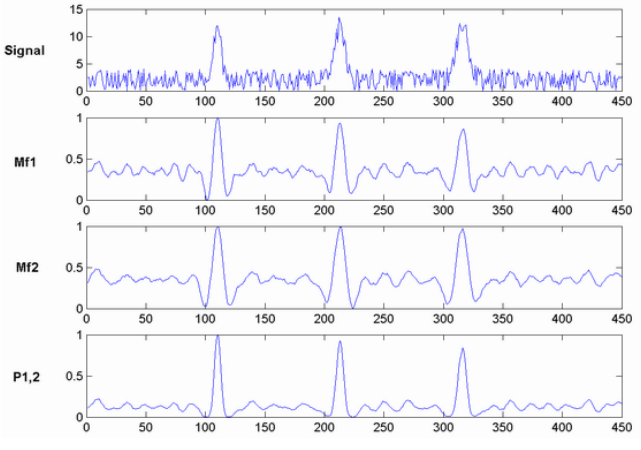

Fig. 6. Multiscale filtering and scale production: Mf1 and Mf2 are the responses at two different scales, P1,2 is their production

According to our experience, the palm vein widths in our infrared images vary from 10 pixels to 20 pixels that corresponding to Gaussian with standard derivation from 1.2 to 2.4. In order to produce strong filter responses, the standard derivation of the matched filters must be similar to the standard derivation of veins. We apply matched filters at two different scales having standard derivation 1.8 and 2.6.

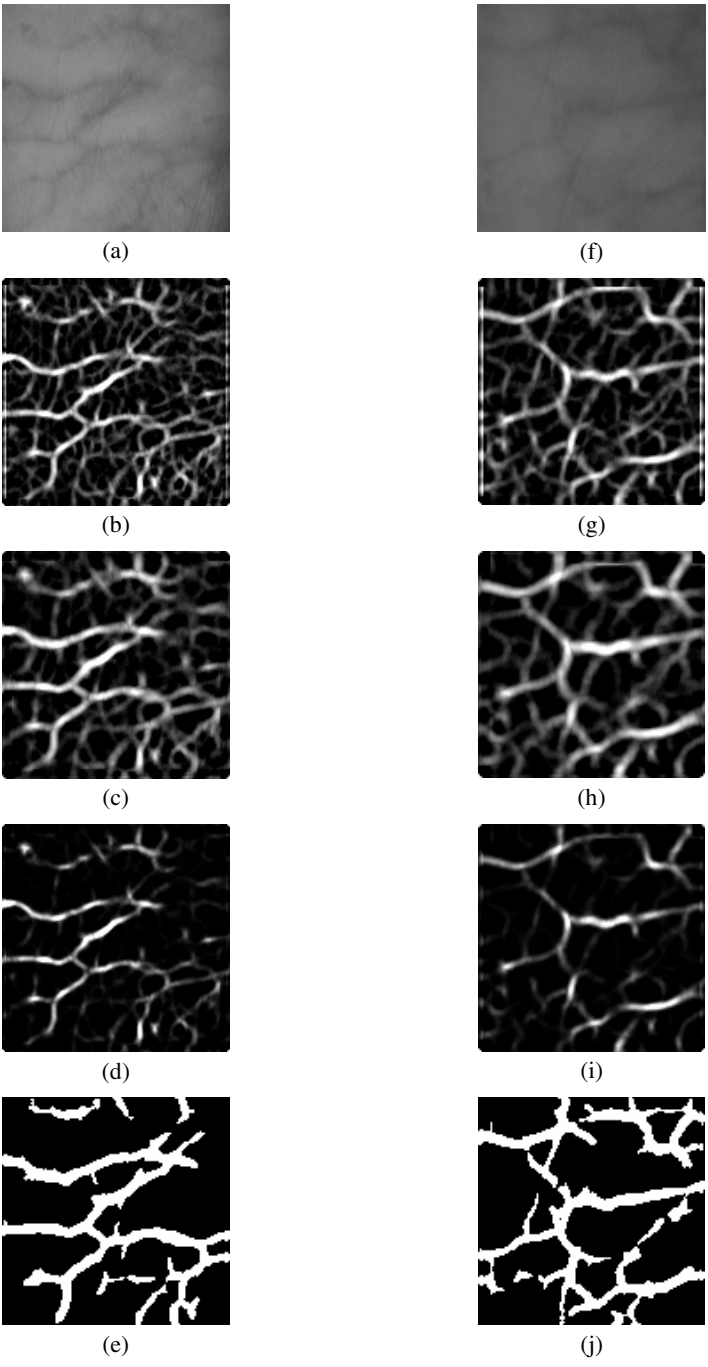

Fig. 7. Thresholding multiscale products: (a) a subimage, (b) & (c) its matched filter responses at two different scales, (d) scale production of (b) & (c), (e) binarized image; (f)~(j) corresponding images of another palm

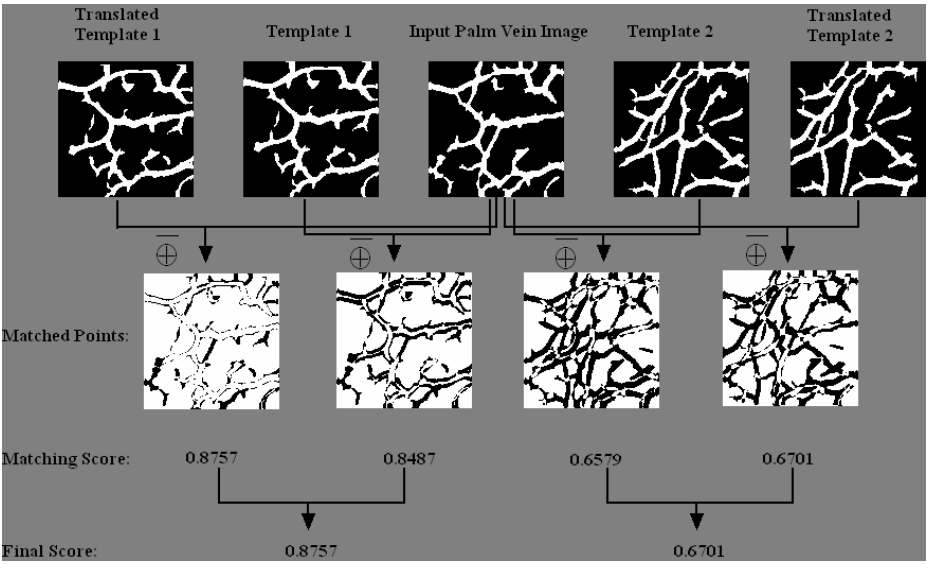

Fig. 8. Matching procedure

There are two reasons for using larger filter standard derivation: (1) Filters with larger size are better at denoising; (2) Reorganization will be more tolerance to rotation and shift. Even the ROI is located by a normalized coordinate, there is still little rotation and shift causing recognized error. In [13], Wu proposed this kind of error can be avoided by dilating the line. The convolution of a Gaussian signal whose standard derivation is σ_1 with a Gaussian filter whose standard derivation is σ_2 will produce a filter response that is a Gaussian whose standard derivation is $\sigma_3 = \sqrt{\sigma_1^2 + \sigma_2^2}$. With a larger σ_2, the vein will be "dilated".

After multiscale filtering and scale production, the filter responses will be binarized by thresholding the multiscale products [9] [10]. Fig. 7 gives some examples of thresholding multiscale products of infrared palm images. Fig. 7(a) is a subimage of an infrared palm image within ROI; Fig. 7(b) and (c) are matched filter responses at different scales; Fig. 7(d) is the scale production of (b) and (c); Fig. 7(e) is the binarized image of (d). Fig. 7(f)~(i) are the corresponding images of another palm. The lines in the binarized images, which represent palm vein, are used as biometric features in our system. This binarized image is named as palm vein image in the following paper.

4 Palm Vein Matching

Using the palm vein image as palm vein templates (only 0 and 1 in the templates), the similarity of two palm images can be calculated by template matching. Let *T* denote a

prepared template in the database and I denote the palm vein image of a new input palm, we match T and I through logical "exclusive or" operation. The matching score of T and I is calculated as

$$S(T,I) = \frac{1}{M \times N} \sum_{i=1}^{M} \sum_{j=1}^{N} \left[\overline{T(i,j) \oplus I(i,j)} \right] \tag{5}$$

where $M \times N$ is the size of T or I (A and B must be the same size), $\oplus$ is the logical "exclusive or" operation, and $-$ is the logical "not" operation. Even we already registered palm images captured at different times at the step of ROI locating, there may still be little rotation and translation between them. To overcome this problem, we vertically and horizontally translate the template T a few points. The final matching score is taken to be the maximum matching score of all the translated positions. This matching procedure is illustrated in Fig. 8.

5 Experimental Results

There are totally 144 infrared palm images in our database. Each of 24 individuals has 6 images. Figure 9 shows images of a palm captured at different times, where the image quality is good. Figure 10 shows images of a palm captured at different times, where the image quality is bad. The probability distribution of genuine and imposter

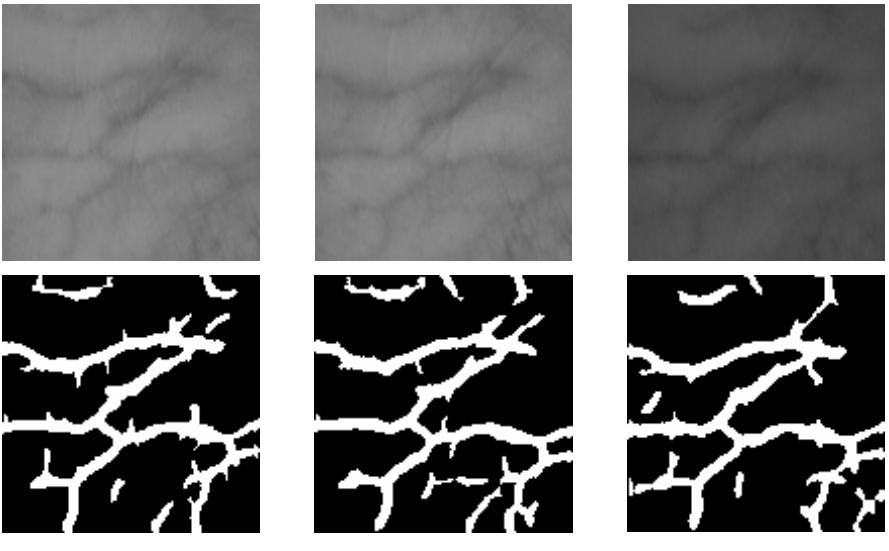

Fig. 9. Images of a palm captured at different times, where the image quality is good. The first row shows the images captured by our device. The second row shows the corresponding vessel extraction results.

is shown in Figure 11. The recognition performance is shown in Figure 12 using ROC curve. We achieved 98.8% recognition rate where the false acceptance rate is 5.5%. Most of the false recognitions were caused by the images of poor quality.

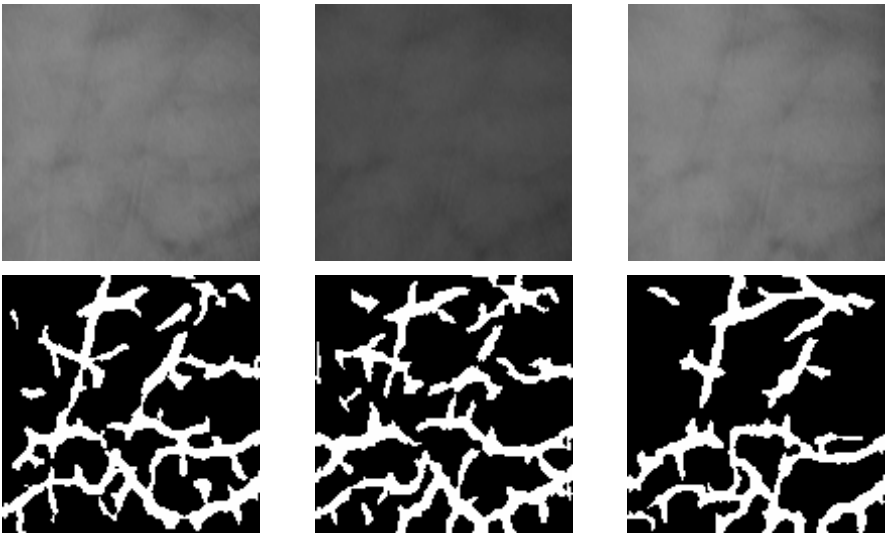

Fig. 10. Images of a palm captured at different times, where the image quality is bad. The first row shows the images captured by our device. The second row shows the corresponding vessel extraction results.

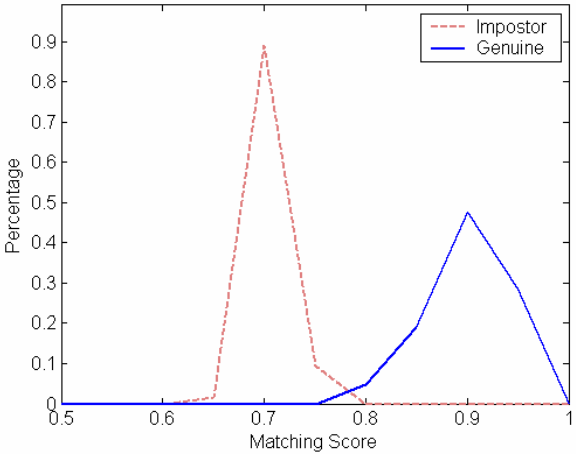

Fig. 11. The probability distribution of genuine and imposter

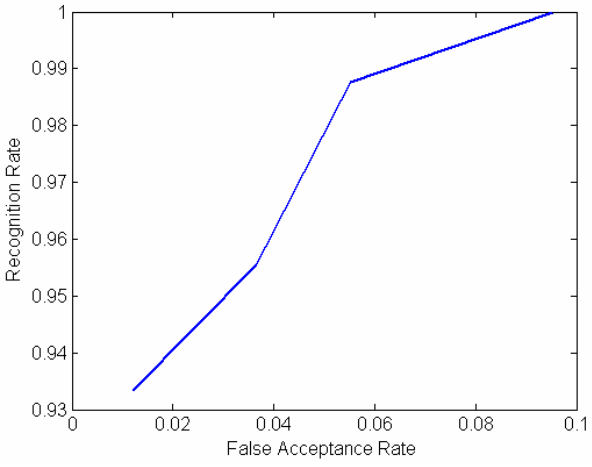

Fig. 12. System performance evaluation using ROC curve

6 Conclusion and Future Work

We proposed a personal identification system using palm vein biometrics to detect the liveness of a person. A low cost CCD camera and a set of infrared light source are used to capture the infrared palm images. A subimage is extracted by locating ROI in terms of image registration. The vein within ROI is used as biometric features to do recognition. The experimental results demonstrate that the recognition rate of our system is fine but not good enough to be a real system.

At present, our capture device is very sensitive to the outside lights. The outside lights can affect the inside infrared light source so that some images have very poor quality. If the capture device can be improved, the system performance should be better. Further, our database is too small to be convincible. More data are required to be collected for the evaluation of our system.

References

1. Lin, C.L., Fan, K.C.: Biometric Verification Using Thermal Images of Palm-Dorsa Vein Patterns. IEEE Transactions on Circuits and Systems for Video Technology 14(2), 199–213 (2004)
2. Fan, K.C., Lin, C.L: The Using of Thermal Images of Palm-dorsa Vein-patterns for Biometric Verification. In: IEEE ICPR, IEEE Computer Society Press, Los Alamitos (2004)
3. Yan, K.W., Zhang, Z.Y., Zhuang, D.: Hand Vein Recognition Based on Multi Supplemental Features of Multi-Classifier Fusion Decision. In: IEEE ICMA, IEEE Computer Society Press, Los Alamitos (2006)
4. Wang, L., Graham, L.: Near- and Far- Infrared Imaging for Vein Pattern Biometrics. In: IEEE ICAVSS, IEEE Computer Society Press, Los Alamitos (2006)

5. Toh, K., Eng, A.H.L., Choo, Y.S., Cha, Y.L., Yau, W.Y., Low, K.S.: Identity Verification Through Palm Vein and Crease Texture. In: IEEE ICB, pp. 546–553. IEEE Computer Society Press, Los Alamitos (2006)
6. Zhang, D., Kong, W.K., You, J., Wong, M.: Online Palmprint Identification. IEEE Trans. on Pattern Analysis and Machine Intelligence 25(9), 1041–1050 (2003)
7. Chaudhuri, S., Chatterjee, S., Katz, N., Nelson, M., Goldbaum, M.: Detection of blood vessels in retinal images using two-dimensional matched filters. IEEE Trans. on Medical Imaging 8, 263–269 (1989)
8. Hoover, A., Kouznetsova, V., Goldbaum, M.: Locating blood vessels in retinal images by piecewise threshold probing of a matched filter response. IEEE Trans. on Medical Imaging 19(3), 203–210 (2000)
9. Bao, P., Zhang, L.: Noise Reduction for Magnetic Resonance Image via Adaptive Multiscale Products Thresholding. IEEE Trans. on Medical Imaging 22, 1089–1099 (2003)
10. Bao, P., Zhang, L., Wu, X.L.: Canny Edge Detection Enhancement by Scale Multiplication. IEEE Trans. Pattern Analysis and Machine Intelligence 27(9) (2005)
11. Li, Q., You, J., Zhang, L., Zhang, D., Bhattacharya, P.: A New Approach to Automated Retinal Vessel Segmentation Using Multiscale Analysis. In: IEEE ICPR, IEEE Computer Society Press, Los Alamitos (2006)
12. Mallat, S., Zhong, S.: Characterization of signals from multiscale edges. IEEE Trans. Pattern Analysis and Machine Intelligence 14, 710–732 (1992)
13. Wu, X., Zhang, D., Wang, K.: Palm Line Extraction and Matching for Personal Authentication. IEEE Transactions On Systems, Man, and Cybernetics, Part A 36(5), 978–987 (2006)